Article

Water-in-Oil Pickering Emulsions Stabilized by Divalent Metal Phenylphosphonate Particles

*Vitor V. S. Machado,[a] Lilian Fernanda M. do Amaral,[a] Anne Raquel Sotiles,[a] Rilton A. de Freitas [a,b] and Fernando Wypych *,[a]*

[a]Departamento de Química, Centro Politécnico, Universidade Federal do Paraná, Jardim das Américas, CP 19032, 81531-980 Curitiba-PR, Brazil

[b]Departamento de Farmácia, Setor de Ciências da Saúde, Universidade Federal do Paraná, Jardim Botânico, CP 19005, 80210-170 Curitiba-PR, Brazil

Phenylphosphonates of zinc (Zn-PPh), calcium (Ca-PPh) and magnesium (Mg-PPh) were synthesized by the hydrothermal method. Samples showed characteristic X-ray diffraction (XRD) patterns of layered compounds with basal spacing in the range of 14-15 Å. According to Fourier transform infrared spectroscopy (FTIR), all compositions showed the presence of characteristic bands attributed to phenyl aromatic rings, phosphonate and lattice metal-oxygen (M−O) vibrations. Different concentrations of phenylphosphonate particles were applied to stabilize water-in-oil Pickering emulsions using vaseline oil in different w/o fractions. The three particle types showed greater affinity for the oil phase (wettability) and the ability to stabilize the emulsions via the Pickering effect. Ca-PPh particles contained a greater emulsified fraction after 20 days of evaluation. This result can be attributed to the particle morphology observed by scanning electron microscopy (SEM). The fibrous morphology of Ca-PPh particles is believed to increase the steric hindrance effect at the surface around the droplets, while the Zn-PPh and Mg-PPh layered particles tended to form clusters.

Keywords: water-in-oil emulsion, Pickering emulsion, layered and fibrous phenylphosphonates

Introduction

Hydrated divalent metal phosphonates are compounds with the general formula $M(O_3PR)\cdot H_2O$ or $M(HO_3PR)_2\cdot H_2O$, where M represents the divalent metal (normally Mn, Co, Zn Ca, etc.) and R represents H, *n*-alkyl or aryl groups.[1-7] In the case of phenylphosphonates, R represents the species $−C_6H_5$, resulting in hydrated compounds with the formula $M(O_3PC_6H_5)\cdot H_2O$ or $M(HO_3PC_6H_5)_2\cdot H_2O$, and in the anhydrous form $M(O_3PC_6H_5)$ or $M(HO_3PC_6H_5)_2$.[8] The water molecules of the hydrated phosphonates are readily removed from the structure and the resulting anhydrous compounds are stable until relatively high temperatures.[2]

Most divalent metal phenylphosphonates are isostructural in composition, where the divalent metal is six-coordinated to two phosphonate oxygens at two opposite faces of the octahedra. In $M(O_3PR)\cdot H_2O$, phosphorous is coordinated to three oxygen atoms of the octahedra and all are coordinated to the $−C_6H_5$ moieties. The octahedra are connected at the corners, forming layers that are packed along the basal directions. All the surfaces of the particles are populated with the organic species $−C_6H_5$, attributing the hydrophobic character to the material.

Figure 1 shows the schematic representation of a generic anhydrous divalent metal phenylphosphonate
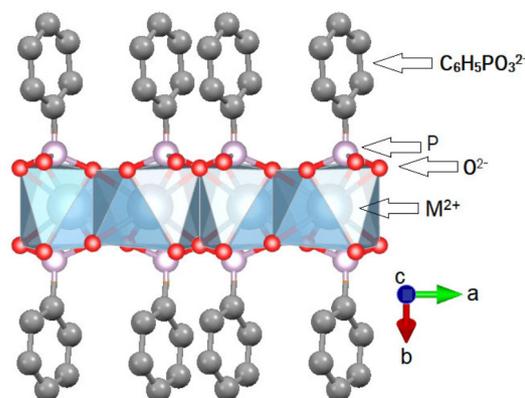

Figure 1. Schematic representation of a generic divalent metal phenylphosphonate structure oriented along the indicated axis.[9]

*e-mail: wypych@ufpr.br
Editor handled this article: Fernando C. Giacomelli (Associate)

$(M^{2+}(O_3PC_6H_5))$, similar to those reported for $(Ca(O_3PC_6H_5))$.[9]

The structure is oriented along the indicated axis and was built using the VESTA (visualization for electronic and structural analysis) program, version 3.4.8.[10]

This class of compounds, due to the inorganic layered core and layered surfaces populated with organic moieties, has properties that are similar to other inorganic layered materials like layered double hydroxides with organic functionalized surfaces, but are obtained in a single step,[7,11] with affordable chemicals along with controllable particle sizes and morphology, giving them potential for application in different industrial areas. Despite the many applications reported previously,[7] as far as we know, this rich class of inorganic-organic hybrid materials, specifically anhydrous layered Zn and Mg phenylphosphonate and fibrous Ca phenylphosphonate, has never been used for stabilization of Pickering emulsions, the objective of the present work.

Experimental

Synthesis of phenylphosphonate particles

For the synthesis of metal phenylphosphonates (M-PPh), analytical grade reagents were used: zinc (99.5%, Êxodo Científica, Sumaré, Brazil), calcium (99.5%, Reatec, Colombo, Brazil) and magnesium (100%, Alphatec, São José dos Pinhais, Brazil) nitrates; phenylphosphonic acid ($C_6H_7O_3P$) (98%, Sigma-Aldrich, Saint Louis, USA); and ammonium hydroxide (NH_4OH) (28%, Êxodo Científica, Sumaré, Brazil). The phenylphosphonate samples were synthesized with adaptation of the methods previously reported in the literature.[12-14] The metal nitrate salt and phosphonic acid were dissolved in 100 mL of purified water by Milli-Q system (Merck, Darmstadt, Germany) and kept under stirring at room temperature. A 10% v/v NH_4OH solution was added to this solution until obtaining a pH value in the range of 5.5-6.0.

The chemical compositions and pH values used in the synthesis of the samples are reported in Table 1. For hydrothermal synthesis, the dispersion was transferred to a round-bottomed flask and remained in a glycerin bath

at 70 °C in a reflux system with a condenser for 24 h. Subsequently, the materials were centrifuged at 4000 rpm (centrifugal force of 2125 G) (Sigma Laborzentrifugen, An der Unteren Söse, Germany), the solution was removed, and a new portion of purified water was added to the slurry, which was redispersed in an ultrasonic bath for several seconds. The process was repeated at least five times. The materials were dried at 60 °C for 48 h, obtaining M-PPh (M = Zn, Ca and Mg).

Characterization of phenylphosphonate particles

For X-ray diffraction (XRD) analysis, samples were deposited in a glass sample holder after the last washing and allowed to dry at room temperature. The analysis was performed using a Shimadzu XRD-6000 diffractometer (Shimadzu, Kyoto, Japan) with Cu Kα = 1.5418 Å radiation, operating with a current of 30 mA, voltage of 40 kV and dwell time of 2° min^{-1}.

Fourier transform infrared (FTIR) spectra were obtained in transmittance mode using KBr pellets containing about 1% of the sample, which were gently mixed and pressed at 6 tons, using a Shimadzu SSP-10A hydraulic press (Shimadzu, Kyoto, Japan). The pellets were analyzed in a Bruker Vertex 70 spectrophotometer (Bruker, Billerica, USA) and the spectra were collected from 400-4000 cm^{-1}, with 32 scans and resolution of 2 cm^{-1}.

Scanning electron microscopy (SEM) and energy dispersive spectroscopy (EDS) were performed with a Tescan Vega3LMU microscope (Tescan, Brno, Czech Republic) with AZtec software.[15] The samples were deposited on copper tapes, and after the EDS analyses were sputtered with a thin gold layer for the SEM analyses.

Elements were quantified by inductively coupled plasma optical emission spectrometry (ICP-OES) with a Thermo Scientific spectrometer model iCAP 6500 (Thermo Fischer Scientific, Waltham, USA) with axial view and the software Thermo Scientific iTeVa version 1.2.0.30.[16] The samples were prepared in triplicate, dissolved in a solution containing 1.0% v/v of nitric acid (HNO_3) (65%, Neon, Suzano, Brazil) in purified water (Milli-Q system) and the data were collected by the equipment in duplicate.

Table 1. Concentration of solutions and synthesis conditions

Compound	$M^{2+}(NO_3)_2$ / mmol	$C_6H_7O_3P$ / mmol	Initial pH	Final pH after adding NH_4OH	Final pH after 24 h at 70 °C
Zn-PPh	12.026	12.003	1.49	5.49	4.39
Ca-PPh	12.998	13.019	1.68	5.51	5.20
Mg-PPh	13.872	13.877	1.37	5.92	4.10

PPh: phenylphosphonates.

Preparation and characterization of emulsions

Water-in-oil (w/o) emulsions were prepared by dispersing 0.1, 0.5 or 1.0 wt.% of the particles in liquid vaseline oil, using oil mass fractions of 0.3, 0.5 or 0.7 and topping up with purified water (Milli-Q system). Then, these mixtures were sonicated with a Misonix Sonics Vibra Cell probe model SM0220 (Misonix, Farmingdale, USA) for one minute at an amplitude of 40% and constant temperature of 25 °C.

After preparation, emulsions macroscopic examination was performed by obtaining photographs in function of time for up to 20 days. In addition to this evaluation, the emulsified volume was measured digitally using the Image J software[17] and compared between the different oil fractions and particle concentrations.

The emulsions were tilted to 45° to observe their flow behavior, and rheological studies were performed using the TA Instruments rheometer model HR-10 (TA Instruments, New Castle, USA) equipped with a cone geometry (40 mm in diameter and 350 mm in the gap). Measurements were carried out at a constant temperature of 25 °C, controlled by a thermostatic bath. Oscillatory stress sweeps were performed from a stress amplitude (τ) of 0.01 to 200 Pa at a frequency of 1 Hz, where the elastic modulus (G') and viscous modulus (G'') vs. stress amplitude were recorded. 1 Pa stress and frequency of 1 Hz, within the linear viscoelastic regime for all tested emulsions, was demonstrated.

Apparent contact angle analyses were performed with a DataPhysics OCA 15 Plus tensiometer (DataPhysics, Filderstadt, Germany) using the sessile drop method. To measure the contact angle, pellets with 12 mm diameter were made using 300 mg of zinc (Zn-PPh), calcium (Ca-PPh) or magnesium (Mg-PPh) phenylphosphonate particles in their powder form and a manual hydraulic press Carver model C (Carver, Wabash, USA) by applying a compaction force of five tons for approximately one minute. The static contact angle between the pellets and a two μL droplet of purified water (Milli-Q system) was measured at least three times and on three different pellets. The contact angle was determined using the SCA 20 Data Physics software.[18]

The emulsions dispersed and continuous phase were analyzed by confocal microscopy as well as their droplets shape and size. Confocal microscopic images of emulsions were obtained using a Nikon confocal laser microscope model AR1+ (Nikon, Tokyo, Japan) with magnifications of 200×. For these analyses, samples were placed in a three-well chamber, particles were labeled with 2.5 ppm of rhodamine (fluorescent red particles with 553 nm excitation and 627 nm emission) (100%, Sigma-Aldrich, Saint Louis, USA) and, for contrast purposes, the aqueous phase was labeled with 2.5 ppm fluorescein (green fluorescent aqueous phase with 490 nm excitation and emission at 514 nm) (100%, Thermo Fischer Scientific, Waltham, USA).

Results and Discussion

Characterization of phenylphosphonate nanoparticles

Since the same number of moles of phenylphosphonic acid and divalent metal salts were used, the expected formula of the obtained compounds was $M(O_3PC_6H_5)$ (M = Zn, Ca, Mg), but the quantitative analysis by ICP-OES (Table 2) indicated that the content of phosphorous was higher than that of the corresponding metals, suggesting contamination with $M(HO_3PC_6H_5)_2$. Most of the publications related to the synthesis of the divalent metal phenylphosphonates with the formula $M^{2+}(O_3PC_6H_5)$ occur in pH in the range of 5 to 6.[2,5,7] As during the hydrothermal synthesis the pH was raised to improve the crystallinity, part of the anions was again protonated and during the Ostwald ripening process, compounds with the formula $Ca(HO_3PC_6H_5)_2$ were obtained as contaminants and indicated by the higher $PO_3^{2-}:M^{2+}$ molar ratio in the case of Zn-PPh and Ca-PPh. In the case of Mg-PPh, the obtained formula was close to $Mg(O_3PC_6H_5)$, as expected.

Table 2. Composition of the samples obtained by ICP-OES

Compound	M^{2+}	PO_3^{2-}	$PO_3^{2-}:M^{2+}$
Zn-PPh	0.418	0.582	1.392
Ca-PPh	0.361	0.639	1.770
Mg-PPh	0.495	0.505	1.020

ICP-OES: inductively coupled plasma optical emission spectrometry. PPh: phenylphosphonates.

Since the pH after the hydrothermal synthesis was still acidic, another possibility was the formation of a material with the formula $Ca_3(C_6H_5PO_3H)_2(C_6H_5PO_3)_2.yH_2O$,[9,19] but as the $PO_3^{2-}:M^{2+}$ would still be 1.333, even this material must be contaminated with $Ca(C_6H_5PO_3H)_2$. Due to the uncertainties of the real composition of the materials, the yields of the synthesis could not be obtained.

In the XRD patterns (Figure 2A), a series of narrow basal peaks were observed, indicating the orientation of the particles in the basal direction and high crystallinity, typical of layered phenylphosphonates.[20-22] To avoid errors attributed to the low angle peaks, the higher-order basal peaks were used to calculate the basal distances, which were 14.36, 15.28 (15.03) and 14.48 Å for Zn-PPh, Ca-PPh

and Mg-PPh, respectively. These data are consistent with the literature and have been attributed to anhydrous phenylphosphonates,[21,22] but in the case of Ca-PPh, a mixture of $Ca(HO_3PC_6H_5)_2$ and $Ca(O_3PC_6H_5)$ was observed (see insert in Figure 2A), as indicated by the splitting of the basal peaks. Studies[19,23] have previously reported that metals such as Mg and Zn tend to form $M(O_3PC_6H_5)$ structures, while calcium forms both $Ca(O_3PC_6H_5)$ and $Ca(HO_3PC_6H_5)_2$, with the estimated formula $Ca_3(C_6H_5PO_3H)_2(C_6H_5PO_3)$.$yH_2O$.

The FTIR spectra of the samples (Figure 2B) showed similarities, with the presence of characteristic stretching bands of the O−H bond in the region from 3600 to 3400 cm^{-1} and water bending in the region of 1620 cm^{-1}.[24,25] Two bands referring to the C−H bond were visible in the region from 3060 to 3000 cm^{-1}, corresponding to the asymmetric and symmetrical stretching, respectively. In turn, bands in the region from 1390 to 1300 cm^{-1} referred to C−H bond bending.[26] The C−C and C=C bond signals of the aromatic ring were observed at 1485 cm^{-1} and in the region of 750-660 cm^{-1}, respectively.[14,27]

The vibration of the phosphorus bound to phenyl group (P−C) was observed at 1435 cm^{-1} and M−O below 450 cm^{-1}.[28,29] Phosphonate has four vibration modes, v_1, v_2, v_3, and v_4, which correspond to symmetrical stretching (v_{sym}), symmetrical bending (δ_{sym}), asymmetrical stretching (v_{asy}) and asymmetric bending (δ_{asy}), respectively.

In general, the samples showed bands in the region from 900 to 1150 cm^{-1} and in the region from 1160 to 1275 cm^{-1}, corresponding to the symmetrical (v_1) and asymmetrical (v_3) stretching of the P−O and O−P−O vibrations, respectively. Other bands were identified in the region below 600 cm^{-1}, attributed to symmetrical (450-530 cm^{-1}) and asymmetrical flexion from 530 to 600 cm^{-1}.[14,25-27,30]

The sample Ca-PPh had the greatest number of bands in the regions of the P−O vibrations (470 to 600 cm^{-1}

and 900 to 1300 cm^{-1}). This was due to the calcium phenylphosphonate synthesis, which formed a mixture of $Ca(HO_3PC_6H_5)_2$ and $Ca(O_3PC_6H_5)$, also indicated by the higher proportion of phosphorous by ICP-OES. This mixture increased the number of bands due to extra vibrations in both structures, and the existence of P−O−H hydrogen vibrations was confirmed by the broad signal in the region from 2200 to 2300 cm^{-1} (Figure 2Bb).[31,32]

The SEM images obtained at different magnifications of zinc (Figures 3a, 3d) and magnesium (Figures 3c, 3f) particles presented similarities, with characteristic morphology of layered compounds, with platelet-like particles having micrometric width and length and nanometric thickness. Phenylphosphonate particles synthesized with different divalent metals also showed platelet-like morphology, such as samples with magnesium, strontium and barium.[33] The sample Ca-PPh had morphology in the form of fibers with different particle sizes and thicknesses (Figures 3b, 3e), in accordance with previously reported results.[9,33]

Characterization of Pickering emulsions

Emulsions containing vaseline oil fractions (Φ_o) ranging from 0.3 to 0.7 in water with increasing particle concentration previously dispersed in the oil phase were prepared. The three different hydrophobic particles Zn-PPh, Ca-PPh and Mg-PPh were analyzed for the first time as stabilizers in water-in-oil (w/o) or oil-in-water (o/w) Pickering emulsions.

Macroscopic analysis

Different tube profiles prepared with and without particles were evaluated after 20 days (Figure 4). The three analyzed particles were white, and as we increased
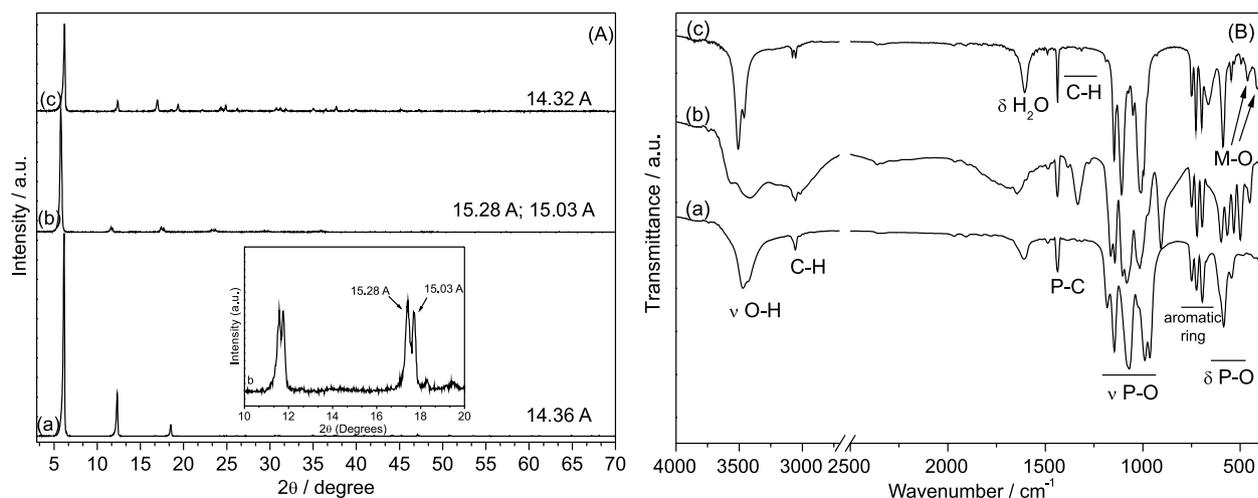

Figure 2. (A) XRD patterns and (B) FTIR (KBr) spectra of Zn-PPh (a), Ca-PPh (b), and Mg-PPh (c).
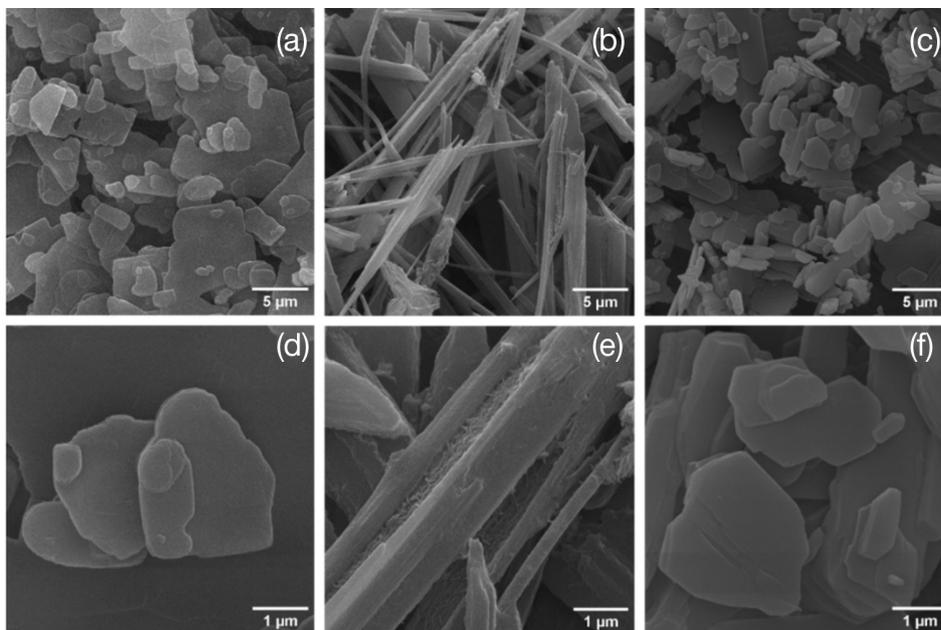
Figure 3. SEM images with magnifications of 10 and 50k×, respectively, of Zn-PPh (a, d), Ca-PPh (b, e), and Mg-PPh (c, f).

the content of these particles in the formulation, greater packing of the emulsified fraction was observed in all formulations. To investigate the emulsions long-term stability, macroscopic images were taken right after emulsion preparation and up to 20 days (Figure S1, Supplementary Information (SI) section).

Macroscopic studies (Figure 4) showed that the emulsified portion increased after sonication as raising particle concentration. With more particles available at the interface between the liquids, the droplet coverage increases, and a well-packed layer of particles becomes more efficient in avoid droplet-to-droplet contact,[34,35] improving emulsion coalescence stability.

The system containing Ca-PPh particles had a larger emulsified portion for up to 20 days of evaluation. In this case, the emulsified volume was higher (total tube volume) in the Φ_o of 0.7 with 1 wt.% of particles. This

higher emulsion stability with Ca-PPh particles may have been caused by the particle fibrous morphology,[36] which in addition to better covering the interface region, might favor the formation of a network at the water-drop interface.[37] In a study using nanocellulose, the same tendency was observed, with similar particle morphology.[38] On the other hand, similar emulsified volumes were noticed when using Zn-PPh or Mg-PPh, which had similar particle sizes and shapes.

To clarify the reason why Ca-PPh stabilized emulsions presented in a higher volume fraction, we studied the emulsions flow behavior using dynamic oscillatory analysis (Figure 5, SI section).

All oil fractions, particle concentrations and particles were compared at the same tension (1 Pa) and frequency (1 Hz), for sake of clarity, under linear viscoelastic regime. Emulsions prepared with Ca-PPh, independently of particle
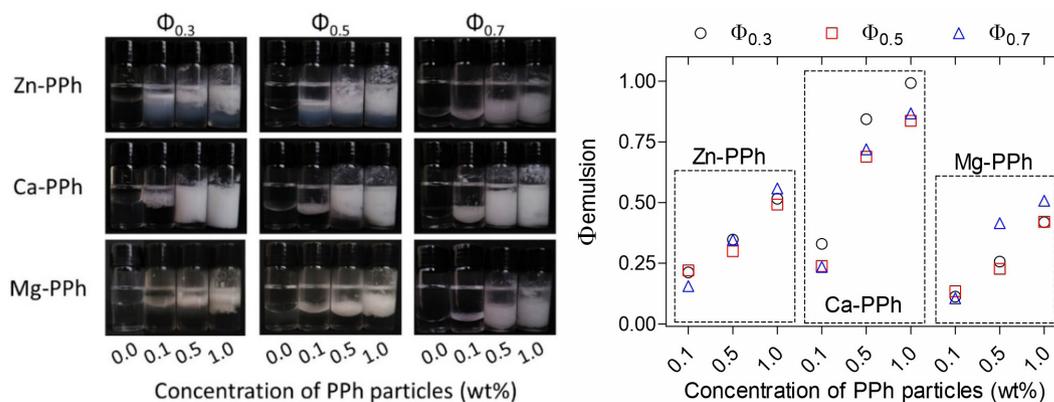

Figure 4. Emulsified portion (Φ) of the tubes 20 days after sonication with Ca-PPh, Zn-PPh and Mg-PPh particles in three different oil-in-water fractions (0.3, 0.5 and 0.7) and particle concentrations ranging from 0.1 to 1 wt.%.
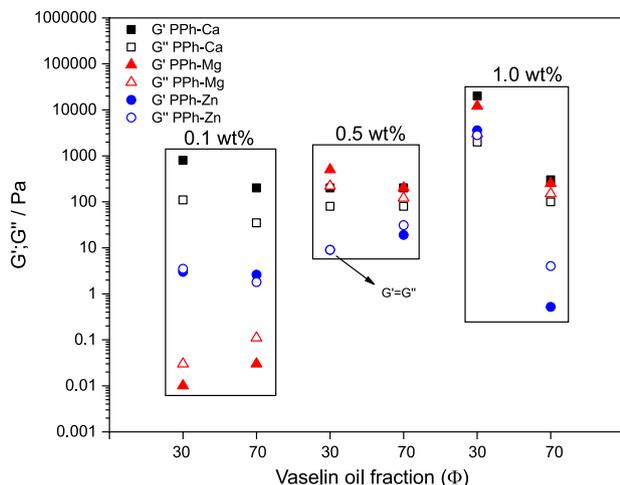
Figure 5. Rheological dynamic oscillatory analysis of emulsions stabilized with Ca-PPh, Zn-PPh and Mg-PPh with Φ = 0.30 or 30% and 0.70 or 70% in weight.

concentration or oil fraction presented a solid-like behavior (G' > G''). Mg-PPh stabilized emulsions solid-like behavior was evident only at higher particle concentration (0.5 and 1.0 wt.%) and Zn-PPh emulsions presented similar values of G' and G'' with equal solid-like and liquid-like behavior. These results are a strong indication that Ca-PPh particles establish a network between them that hinders or inhibits droplet coalescence (Figure 5).

Vaseline oil presented higher wettability in the three systems studied (with a contact angle close to 15°, see Table S1, SI section). Partial wettability of water was confirmed by the analysis of the particle-water-air contact angle (Figure 6).

Hydrophobic particles projected less in the aqueous phase (Figure 6), forming a particle-water-air contact angle greater than or close to 90º, which tended to form a water-in-oil (w/o) emulsion. This behavior was expected for all particles at contact angles of 75.9 ± 7.5º for Ca-PPh, 76.2 ± 4.1º for Mg-PPh and 90.3 ± 3.7º for Zn-PPh. According to the literature,[39] values close to 90º correspond to the maximum anchoring energy of the particles at the interface. Due to the amphiphilic character of these

particles, they presented greater potential for stabilizing w/o emulsions.[40]

Measurements of three-phase angle between a water droplet on a particle layer immersed in a continuous oil phase generated high contact angles with the interface for all particles evaluated (Ca-PPh, θ = 130.5 ± 10.8°, Mg-PPh, θ = 133.2 ± 5.2° and Zn-PPh, θ = 147.6 ± 4.1°). These values remained constant for up to 20 min, indicating that the particles were preferentially wetted by the oil, not by the water phase. Interfacial tension measurements were not performed since samples are turbid even at lower concentrations (0.1 wt.%).

If the particles had been completely wetted by water or oil, they would have remained dispersed in that phase and no stable emulsion would have been obtained. The results obtained indicated that the particles had greater affinity for the oily phase than for the aqueous phase. This behavior was expected because the layered structure of phenylphosphonate particles exhibits aromatic rings on their surfaces, which are composed of non-polar molecules that have a hydrophobic character like other compounds.[41] Thus, we expected the vaseline oil to be the continuous phase in the emulsions, according to the Finkle rule.[42]

Confocal microscopic analysis of emulsions

In the microscopic images of the water-in-oil emulsion stabilized by phenylphosphonate particles (Figure 7), it was possible to observe rhodamine-labeled particles (red color) in all emulsions at the drop interface, confirming the Pickering effect, while the fluorescein-labeled water (green color) indicated the dispersed phase.

As expected, the emulsions containing Zn-PPh, Ca-PPh and Mg-PPh (Figure 7) formed water-in-oil emulsions in all formulations containing 1 wt.% of particles, but in the Ca-PPh formulation (Figure 7b), the type of emulsion formed was influenced by the oil fraction (Φ_o = 0.3).

Apparently, the stabilization was associated with a dual mechanism, increase of the continuous phase viscosity and
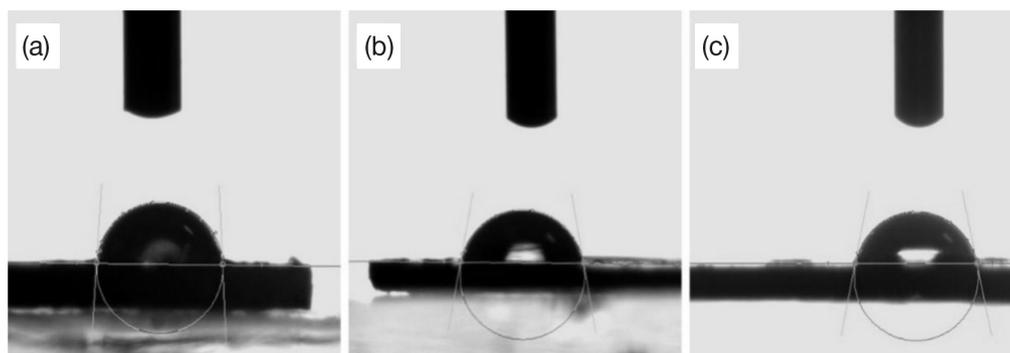

Figure 6. Contact angle measurements of droplets of water on pellets of hydrophobic Zn-PPh (a), Ca-PPh (b) and Mg-PPh (c).

Pickering effect. Low concentrations of the anisotropic fibrous particles promoted some phase inversion and required a higher concentration than the other two layered particles. The lowest concentration of particles (0.1 and 0.5 wt.%) for up to 3 h after preparation (Figure S3, SI section) caused the formation of a w/o emulsion even when using Φ_o 0.3 and stabilization with Ca-PPh particles. This clearly demonstrated that the addition of low contents of these fibrous particles was not able to promote the coverage and continuous phase viscosity necessary to produce kinetic stabilization of the o/w emulsion. The increase of oil in the Zn-PPh formulation (Figure 7a) led to an increase in droplet size. In the intermediate oil fraction (Φ_o of 0.5), the drops started to coalesce and in the oil fraction of 0.7 some vesicles formed and remained intact until 72 h after preparation. In contrast, large w/o drops (> 100 μm) were observed for the Mg-PPh formulation (Figure 7c) in all oil fractions, and in all the w/o emulsions, a thick layer of particles was observed at the interfaces.

Despite being structurally similar, the fibrous Ca-PPh and layered Zn-PPh and Mg-PPh presented different interactions with the interface. This effect can be attributed to the better positioning of Ca-PPh on the droplet surfaces, demanding a lower concentration for stabilization, leading to its long-term stability. In contrast, layered particles of Zn-PPh and Mg-PPh became aggregated, hindering the interface adsorption between the emulsion phases.

When fibrous particles were sonicated at high energy, some disassembly of large fibers bundles into smaller sizes occurred (Figure S4, SI section), allowing better adsorption of these smaller particles with fibrous geometry on the liquid interface. This is consistent with the confocal images, where emulsions containing Ca-PPh formed a greater number of droplets with smaller diameters than the Zn-PPh and Mg-PPh system, which had large drops and a layer of thicker particles at the interface (agglomerated particles).

Other fibrous-shaped particles, such as cellulose nanocrystals,[42] polystyrene ellipsoids,[43] gold and silica nanowires,[44] and platelet-like particles such as layered double hydroxides,[45,46] laponite clay,[47,48] and kaolinite,[49] have shown high stability than spherical particles. The effects of length, concentration and wettability of
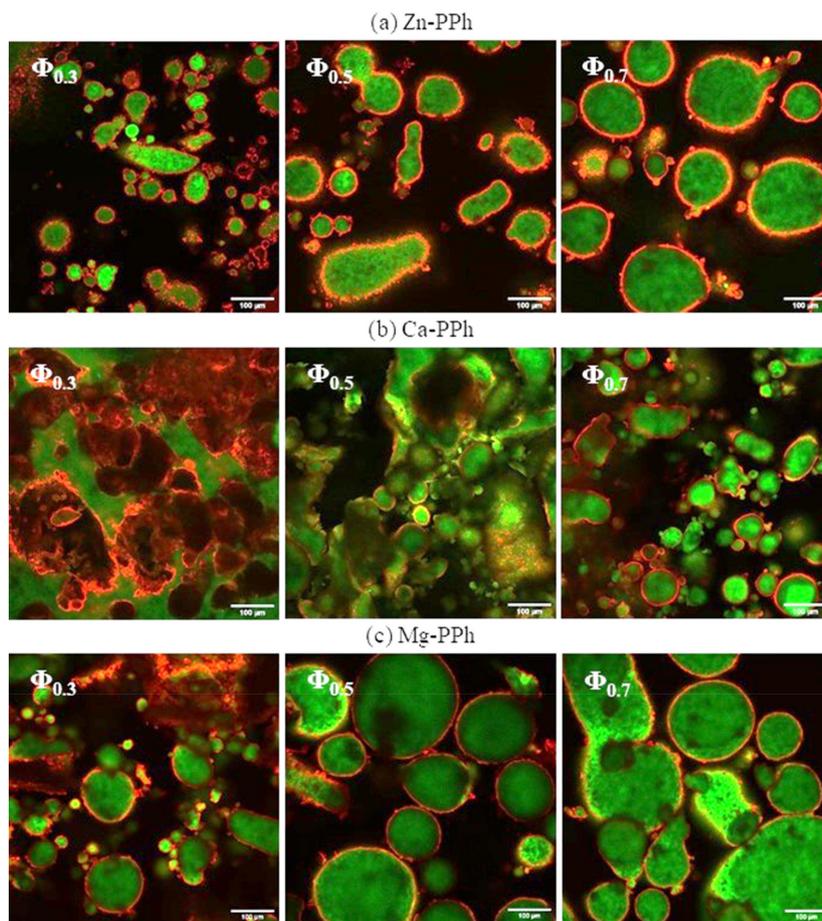

Figure 7. Confocal fluorescence microscopic image of emulsions containing oil and ultrapure water (Φ_o ranging from 0.3-0.7) and 1.0 wt.% of particles of Zn-PPh (a), Ca-PPh (b) and Mg-PPh (c), 72 h after preparation (200× magnification). The particles were stained with rhodamine B (2.5 ppm) and fluorescein (2.5 ppm) was used to stain the water. The scale bar is fixed at 100 μm.

hydrophilic and hydrophobic silica nanowires in oil-in-water or water-in-oil emulsion stabilization were recently reported.[50] The authors suggested that increasing the length or concentration of silica nanowires resulted in better performance in stabilizing the dispersed phase due to the high coverage of the droplet interface achieved. For anisotropic particles, strong capillary interactions arise due to interface deformation caused by a wavy contact line or by particle shape effects.[43,51]

Both layered or more elongated shapes, as well as fibrous ones, can lead to distortion of the interface around them, generating a reduction of free energy when trapped at the liquid-liquid interface.

Conclusions

Phenylphosphonate particles were synthesized by the hydrothermal method and XRD indicated a series of narrow basal peaks, typical of layered phenylphosphonates. Basal distances of 14.36, 15.28 (15.03) and 14.48 Å were obtained respectively for Zn-PPh, Ca-PPh and Mg-PPh.

The FTIR spectra presented bands attributed to O–H, C–H, C–C, P–C, C=C vibrations, typical of phenylphosphonates. SEM images revealed layered micrometric dimensions and nanometric thicknesses of particles with Zn-PPh and Mg-PPh and fibrous particles of Ca-PPh.

The results using fibrous (Ca-PPh) and layered (Zn-PPh and Mg-PPh) particles with the same surface chemistry showed that after stirring, stable droplets were formed in all the systems. Inverse emulsions were obtained using fibrous particles of Ca-PPh in the smallest fraction of oil. Confocal laser microscopic images revealed a densely packed layer of particles on the droplet surface, confirming the Pickering effect.

Furthermore, emulsion stabilization depends on the shape of the particles, where droplet coverage is more effective when using Ca-PPh particles due to the capillary forces induced by its fibrous shape. In addition, the increase in emulsion elastic modulus in the dynamic oscillatory analysis attributed to a network formed by these fibrous particles may also contribute to the highly effective stabilization.

The consumers demand also for eco-sustainable and safer products and the use of Pickering particles brings an alternative strategy to molecular surfactants to stabilize emulsions, reducing the undesirable effects of classical surfactants, enhancing their long-term stability with applications in cosmetic and pharmaceutical products. Metal phosphonate are a promising eco-friendly inorganic/organic hybrid filler with a layered structure been described

as biomaterial in bone implants, as drug delivery system and protein binding. So, these properties associated to emulsion stabilization highlight phenylphosphonate particles as promising Pickering particles candidates.[52-54]

Supplementary Information

Supplementary information (macroscopic images of emulsions as a function of time with different concentrations of particles, tilt test of emulsion stabilized, contact angles, confocal fluorescence microscopic images of emulsions and SEM images) is available free of charge at http://jbcs.sbq.org.br as PDF file.

Acknowledgments

References

1. Cao, G.; Lynch, V. M.; Swinnea, J. S.; Mallouk, T. E.; *Inorg. Chem.* 1990, *29*, 2112. [Crossref]

2. Frink, K. J.; Wang, R. C.; Colón, J. L.; Clearfield, A.; *Inorg. Chem.* 1991, *30*, 1438. [Crossref]

3. Zhang, Y.; Clearfield, A.; *Inorg. Chem.* 1992, *31*, 2821. [Crossref]

4. Poojary, D. M.; Clearfield, A.; *J. Am. Chem. Soc.* 1995, *117*, 11278. [Crossref]

5. Bataille, T.; Bénard-Rocherulle, P.; Louer, D.; *J. Solid State Chem.* 1998, *140*, 62. [Crossref]

6. Clearfield, A.; *Chem. Mater.* 1998, *10*, 2801. [Crossref]

7. Gao, L.-L.; Song, S.-Y.; Ma, J.-F.; Yang, J.; *Cryst. Growth Des.* 2007, *7*, 895. [Crossref]

8. Cunningham, D.; Hennelly, P. J. D.; Deeney, T.; *Inorg. Chim. Acta* 1979, *37*, 95. [Crossref]

9. Kopecká, K.; Beneš, L.; Melánová, K.; Zima, V.; Knotek, P.; Zetková, K.; *Beilstein J. Nanotechnol.* 2018, *9*, 2906. [Crossref]

10. Momma, K.; Izumi, F.; *J. Appl. Crystallogr.* **2011**, *44*, 1272. [Crossref]

11. Wang, J.; Yang, F.; Li, C.; Liu, S.; Sun, D.; *Langmuir* **2008**, *24*, 10054. [Crossref]

12. Poojary, D. M.; Zhang, B.; Cabeza, A.; Aranda, M. A. G.; Brogue, S.; Clearfield, A.; *J. Mater. Chem.* **1996**, *6*, 639. [Crossref]

13. Xu, T.; Wang, Y.; He, D.; Xu, Y.; Li, Q.; Shen, C.; *Polym. Test.* **2014**, *34*, 131. [Crossref]

14. Chen, Y.-A.; Chen, E.-C.; Wu, T.-M.; *J. Mater. Sci.* **2015**, *50*, 7770. [Crossref]

15. *AZtec software*, 2.1; Oxford Instruments, UK, 2013.

16. *iTEVA software*, 1.2.0.30; Thermo Scientific, USA, 2010.

17. Rasband, W.; *ImageJ*, 2.0.0-rc-3; National Institutes of Health, USA, 2014.

18. *SCA20* 4.5.14; Dataphysics Instruments GmbH, Germany, 1997.

19. Svoboda, J.; Zima, V.; Beneš, L.; Melánová, K.; Vlček, M.; *Inorg. Chem.* **2005**, *44*, 9968. [Crossref]

20. Wilke, M.; Kabelitz, A.; Gorelik, T. E.; Buzanich, A. G.; Reinholz, U.; Kolb, U.; Radermann, K.; Emmerling, F.; *Dalton Trans.* **2016**, *45*, 17453. [Crossref]

21. Zhang, Y.; Scott, K. J.; Clearfield, A.; *J. Mater. Chem.* **1995**, *5*, 315. [Crossref]

22. Zima, V.; Svoboda, J.; Beneš, L.; Melánová, K.; Trchová, M.; *Solid State Sci.* **2006**, *8*, 1380. [Crossref]

23. Mahmoudkhani, A. H.; Langer, V.; *Solid State Sci.* **2001**, *3*, 519. [Crossref]

24. Migahed, M. A.; Alsabagh, A. M.; Abdou, M. I.; Abdel-Rahman, A. A.-H.; Aboulrous, A. A.; *J. Mol. Liq.* **2019**, *281*, 528. [Crossref]

25. Bhanja, P.; Mohanty, B.; Paul, B.; Bhaumik, A.; Jena, B. K.; Basu, S.; *Electrochim. Acta* **2022**, *416*, 140277. [Crossref]

26. Palvadeau, P.; Queignec, M.; Venien, J. P.; Bujoli, B.; Villieras, J.; *Mater. Res. Bull.* **1988**, *23*, 1561. [Crossref]

27. Melánová, K.; Beneš, L.; Svoboda, J.; Zima, V.; Trchová, M.; Vlček, M.; Amonasy, N.; *J. Inclusion Phenom. Macrocyclic Chem.* **2017**, *87*, 331. [Crossref]

28. Haky, J. E.; Braddy, J. B.; Dando, N.; Weaver, D.; *Mater. Res. Bull.* **1997**, *32*, 297. [Crossref

29. Pramanik, M.; Bhaumik, A.; *Chem. - Eur. J.* **2013**, *19*, 8507. [Crossref]

30. Stoch, P.; Stoch, A.; Ciencinska, M.; Krakowiak, I.; Sitarz, M.; *J. Non-Cryst. Solids* **2016**, *450*, 48. [Crossref]

31. Mahmoudkhani, A. H.; Langer, V.; Smrcok, L.; *Solid State Sci.* **2002**, *4*, 873. [Crossref]

32. Murugavel, R.; Gogoi, N.; *Bull. Mater. Sci.* **2009**, *32*, 321. [Crossref]

33. Xu, X.-J.; Zhou, L.-H.; Lu, C.-Z.; *Mater. Lett.* **2007**, *6*, 4980. [Crossref]

34. Akartuna, I.; Studart, A. R.; Tervoort, E.; Gonzenbach, U. T.; Gauckler, L. J.; *Langmuir* **2008**, *24*, 7161. [Crossref]

35. Qi, F.; Wu, J.; Sun, G.; Nan, F.; Ngai, T.; Ma, G.; *J. Mater. Chem. B* **2014**, *2*, 7605. [Crossref]

36. Ortiz, D. G.; Bohatier, C. P.; Cambedouzou, J.; Bechelany, M.; Miele, P.; *Engineering* **2020**, *6*, 468. [Crossref]

37. Tervoort, E.; Studart, A. R.; Denier, C.; Gauckler, L. J.; *RSC Adv.* **2012**, *2*, 8614. [Crossref]

38. Kalashnikova, I.; Bizot, H.; Bertoncini, P.; Cathala, B.; Capron, I.; *Soft Matter* **2013**, *9*, 952. [Crossref]

39. Destribats, M.; Gineste, S.; Laurichesse, E.; Tanner, H.; Leal-Calderon, F.; Héroguez, V.; Schmitt, V.; *Langmuir* **2014**, *30*, 9313. [Crossref]

40. Aveyard, R.; *Soft Matter.* **2012**, *8*, 5233. [Crossref]

41. Aveyard, R.; Binks, B. P.; Clint, J. H.; *Adv. Colloid Interface Sci.* **2003**, *100-102*, 503. [Crossref]

42. Finkle, P.; Draper, H. D.; Hildebrand, J. H.; *J. Am. Chem. Soc.* **1923**, *45*, 2780. [Crossref]

43. Madivala, B.; Vandebril, S.; Fransaer, J.; Vermant, J.; *Soft Matter.* **2009**, *5*, 1717. [Crossref]

44. Patra, D.; Malvankar, N.; Chin, E.; Tuominen, M.; Gu, Z.; Rotello, V. M.; *Small* **2010**, *6*, 1402. [Crossref]

45. do Amaral, L. F. M.; Wypych, F.; de Freitas, R. A.; *Appl. Clay Sci.* **2021**, *201*, 105918. [Crossref]

46. Zhang, N.; Zhang, L.; Su, D.; *Langmuir* **2015**, *31*, 4619. [Crossref]

47. Bon, S. A. F.; Colver, P. J.; *Langmuir* **2007**, *23*, 8316. [Crossref]

48. Brunier, B.; Sheibat-Othman, N.; Chniguir, M.; Chevalier, Y.; Bourgeat-Lami, E.; *Langmuir* **2016**, *32*, 6046. [Crossref]

49. Sieben, P. G.; Wypych, F.; de Freitas, R. A.; *Appl. Clay Sci.* **2022**, *216*, 106378. [Crossref]

50. Yan, H.; Zhao, B.; Long, Y.; Zheng, L.; Tung, C.-H.; Song, K.; *Colloids Surf., A* **2015**, *482*, 639. [Crossref]

51. Liu, I. B.; Sharifi-Mood, N.; Stebe, K. J.; *Annu. Rev. Condens. Matter Phys.* **2018**, *9*, 283. [Crossref]

52. Dorozhkin, S. V.; Epple, M.; *Angew. Chem., Int. Ed.* **2002**, *41*, 3130. [Crossref]

53. Bujoli, B.; Lane, S. M.; Nonglaton, G.; Pipelier, M.; Léger, J.; Talham, D. R.; Tellier, C.; *Chem.-Eur. J.* **2005**, *11*, 1980. [Crossref]

54. Jia, C.; Zhou, S.; Xie, Z.; Wang, L.; Yang, Y.; Sun, X.; Xiea, Y.; Yanga, J.; *Polym Int.* **2021**, *70*, 1264. [Crossref]